SUPPORTING INFORMATION

Stability of Polymer Grafted Nanoparticle Monolayers: Impact of Architecture and Polymer-Substrate Interactions on Dewetting

Justin Che[1,2], Ali Jawaid[1,3], Christopher A. Grabowski[1,3], Yoon-Jae Yi[1,4], Golda Chakkalakal Louis[5], Subramanian Ramakrishnan[5], Richard A. Vaia[1]

[1]*Materials and Manufacturing Directorate, Air Force Research Laboratory, WPAFB, OH 45433*
[2]*National Research Council, Washington, D.C. 20001*
[3]*UES, Inc., Dayton, OH 45432*
[4]*College of Science and Mathematics, Wright State University, Dayton, OH 45435*
[5]*College of Engineering, Florida A&M University-Florida State Univ., Tallahassee, FL 32310*

Table of Contents:

S1. EXPERIMENTAL

Synthesis and Characterization of Polystyrene Grafted Gold Nanoparticles (AuNP-PS).

Detailed synthesis for polystyrene grafted gold nanoparticles (AuNP-PS) is available in reference 1. In brief, hydrogen tetrachloroaurate trihydrate ($HAuCl_4 \cdot 3H_2O$) (Sigma Aldrich) and tribasic sodium citrate ($Na_3C_6H_5O_7 \cdot 2H_2O$) (Sigma Aldrich) were added to deionized water at 100 °C and stirred for 15 minutes until the solution turned to a ruby red color. The reaction mixture was then allowed to cool, followed by purification via diafiltration. The resulting solution was functionalized with thiol-terminated polystyrene (Polymer Source, Inc.) in tetrahydrofuran and vigorously mixed for 1 minute. The water and tertahydrofuran mixture was decanted and the remaining materials were redispersed in toluene and centrifuged to remove free polystyrene as confirmed by size exclusion chromatography (SEC).

Table 1 in main text summarizes the characterization of the AuNP-PS with 20 nm core diameters grafted with molecular weights (M_n) 12,000 g/mol, 20,000 g/mol, and 50,000 g/mol thiol-terminated polystyrene (denoted as Au20-PS12k, Au20-PS20k, and Au20-PS50k, respectively). Small-angle X-ray scattering (SAXS) (S-MAX3000, Rigaku) was used to determine the core size of the gold nanoparticles (Figure S1). Thermal gravimetric analysis (TGA) (Q500, TA Instruments) was used to determine the graft density (σ) and the number of chains per PGN (n).

Fabrication of Surface Energy Gradients

Surface energy gradients were prepared following established vapor deposition procedures by Genzer et al.[2-3] Silicon (100) wafers (Ted Pella, Inc.) were cut into 6.4 x 2.5 cm^2 pieces and exposed to ultraviolet-ozone (UVO) treatment for 20 minutes to remove organic contaminants and activate surface hydroxyl groups. The wafers were then sequentially rinsed and sonicated with ethanol, 50 v/v% ethanol:toluene, and toluene to ensure the removal of contaminants and excess

water at the surface. 150 μL of stock *n*-octyltrichlorosilane (OTS) (Gelest, Inc.) were deposited in a small rectangular reservoir that is placed in parallel to the longer edge of the substrate (separation distance of 0.5 cm). The entire system was enclosed in a Petri dish and allowed to react for 5 minutes in ambient conditions. The substrate was subsequently rinsed thoroughly with deionized water to remove physisorbed silane molecules and blown dry with nitrogen. It should be noted that the volume of OTS, reaction time, and separation distance all play a role in the adsorption of OTS. The parameters used here were predetermined to give the largest SE gradient. Contact angles at various positions on the surface energy gradient substrate were measured as discussed below.

Formation of PGN films

Thin films of linear homopolymer PS and monolayers of AuNP-PS were prepared using a custom-built flow-coater. Detailed information about the flow-coater setup, solution properties, and the different regimes of film formation between linear and PGN is available in reference 1. Linear PS films with (M_n) 10,500 g/mol, 20,800 g/mol, and 52,000 g/mol (denoted as PS11k, PS21k, and PS52k, respectively) (Polymer Source, Inc.) were deposited on SE gradient substrates at a constant velocity of 10 mm/s, whereas AuNP-PS films were deposited at 0.5 mm/s. The films produced were approximately 35-40 nm thick as determined by tapping mode atomic force microscopy (AFM) on a Dimension Icon (Bruker Corporation).

Thin Film Dewetting

Following approaches from Ashley et al.[4], a thermal gradient was applied to the thin films orthogonal to the SE gradient using a Kofler hot bench (Wagner & Munz). The temperature was calibrated using a 572CM direct contact spot check surface thermometer (PTC Instruments) and an SC620 forward-looking infrared (FLIR) camera (FLIR Systems) with accuracies up to ±2% of reading. Temperatures at different spots along the substrate were recorded with an average reading

of 7 °C/cm. It should be noted that the temperatures were uniform in the orthogonal direction (parallel to SE gradient) as shown in Figure S2. The thin films were thermally annealed for 1 hour in ambient conditions. The film morphologies at specific positions on the orthogonal SE and temperature gradient were measured using a VK-X260K laser scanning confocal microscope (Keyence) in reflection mode. The determination of stability boundaries were carried out by adjusting the threshold of the optical micrographs using Image J. The presence of dewetted holes and bare substrate after thresholding are termed "unstable". In contrast, the absence of any features after thresholding is labelled as "stable".

Determination of Critical Radius, R_c and $R_{n,PGN}$ for PGNs

The critical radius for a swollen PGN as proposed by Ohno et al.[5] is $R_c = R_0(\sigma_0^*)^{0.5}(\nu^*)^{-1}$, where R_0 is the radius of the NP core, σ_0^* is the reduced grafting density, and ν^* is related to the excluded-volume parameter. Using the structural parameters for the PGNs (Table 1), R_c is Au20-PS12k: 55.2 ± 6.3 nm; Au20-PS20k: 49.9 ± 5.7 nm; Au20-PS50k: 40.8 ± 4.6 nm. These values are for PGNs in theta solvent swelling conditions. Assuming these conditions, the theoretical values for radius of a swollen PGN determined by Ohno is consistent with the radius of the swollen PGN in toluene determined from Dynamic Light Scattering (DLS, Table 1). $R_{n,PGN}$ is the radius of the PGN in the melt (unswollen) state and can be estimated by:

$$R_{n,PGN} = \left(\frac{3V_{n,PGN}}{4\pi}\right)^{1/3} = \left(\frac{3(V_{NP}+V_{PS})}{4\pi}\right)^{1/3} = \left(\frac{3\left(\left(\frac{4\pi R_0^3}{3}\right)+\left(\frac{4\pi R_0^2 \sigma M_W}{\rho_{PS}\, N_A}\right)\right)}{4\pi}\right)^{1/3} \quad \text{(S1)}$$

$$R_{n,PGN} = \left(R_0^3 + \frac{3R_0^2 \sigma M_W}{\rho_{PS}\, N_A}\right)^{1/3} \quad \text{(S2)}$$

where $V_{n,PGN}$ is the volume of the PGN in the unswollen state, V_{NP} and V_{PS} are the volumes of the NP and PS respectively, σ is the graft density, M_w is the molecular weight of PS, ρ_{PS} is the density

of PS, and N_A is the Avogadro's number. Values are summarized in Table 1 and are consistent with previous x-ray studies[1].

Surface and Interfacial Energy Determination

Contact angle measurements using water and ethylene glycol of the substrate and polymer thin films were carried out using sessile drop mode on an Attension Optical Tensiometer (Biolin Scientific). The polymer film is partially soluble in nonpolar solvents and hence, the surface energy of the polymer was confirmed using glycerol as an additional test solvent and found to be identical. The surface energies of the substrate and polymer can be calculated using Owens-Wendt geometric mean approach[6]:

$$\gamma_L(1+\cos\theta) = 2\left(\left(\gamma_S^d\gamma_L^d\right)^{1/2} + \left(\gamma_S^p\gamma_L^p\right)^{1/2}\right) \quad \text{(S3)}$$

where θ is the contact angle, γ is the surface energy, subscripts *S* and *L* denote the solid and test liquids used respectively, and superscripts *d* and *p* denote the dispersive and polar components to the total surface energy. By simultaneously solving for γ_S^d and γ_S^p using the contact angles of two test liquids with known values of γ_L, γ_L^d, and γ_L^p, the total surface energy of the solid component (i.e. substrate and polymer film) can be determined:

$$\gamma_S = \gamma_S^d + \gamma_S^p \quad \text{(S4)}$$

In addition, the interfacial energy between the substrate and polymer (γ_{SP}) can be determined using Fowkes' theory[7-8]:

$$\gamma_{SP} = \gamma_S + \gamma_P - 2\left(\left(\gamma_S^d\gamma_P^d\right)^{1/2} + \left(\gamma_S^p\gamma_P^p\right)^{1/2}\right) \quad \text{(S5)}$$

Temperature dependence of the substrate surface energy gradient to the *n*-octyltrichlorosilane functionalized silicon was determined by measuring the contact angles using ethylene glycol and glycerol directly on the Kofler hot bench (Figure S3). Contact angles along different positions from 130-160°C were converted to γ_S using Equation S3.

Note that the geometric approximation (Equation S3) is more commonly used, and valid, when determining surface energy of neutral to low-charge surfaces (as examined herein). Well characterized test liquids that can be divided into their respective polar and dispersive components are available. In contrast, the acid-base approach[9-10] is more appropriate to calculate surface energies of inorganics and surfaces containing ions. In addition, this approach has a limited number of reference liquids with known values of the acid, base, and dispersive components.

S2. Characterization of AuNP-PS Samples

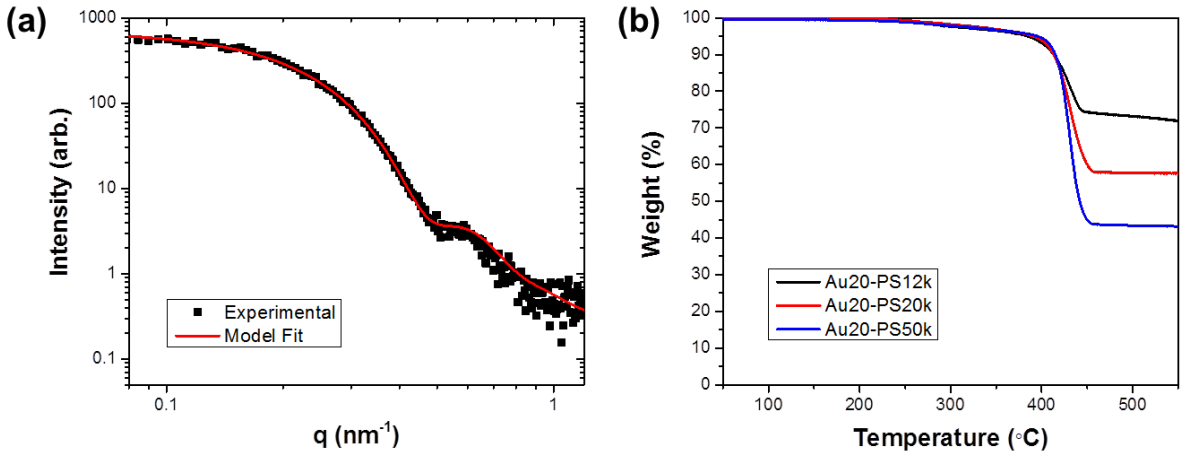

Figure S1 Characterization of gold nanoparticles functionalized with polystyrene (AuNP-PS). (a) SAXS profiles of gold nanoparticle fitted using a Schultz distribution to determine core size and polydispersity (radius = 9.5±1.5 nm). (b) TGA profiles of Au20-PS12k (black), Au20-PS20k (red), and Au20-PS50k (blue) to determine grafting densities.

S3. Orthogonal Surface Energy and Temperature gradients

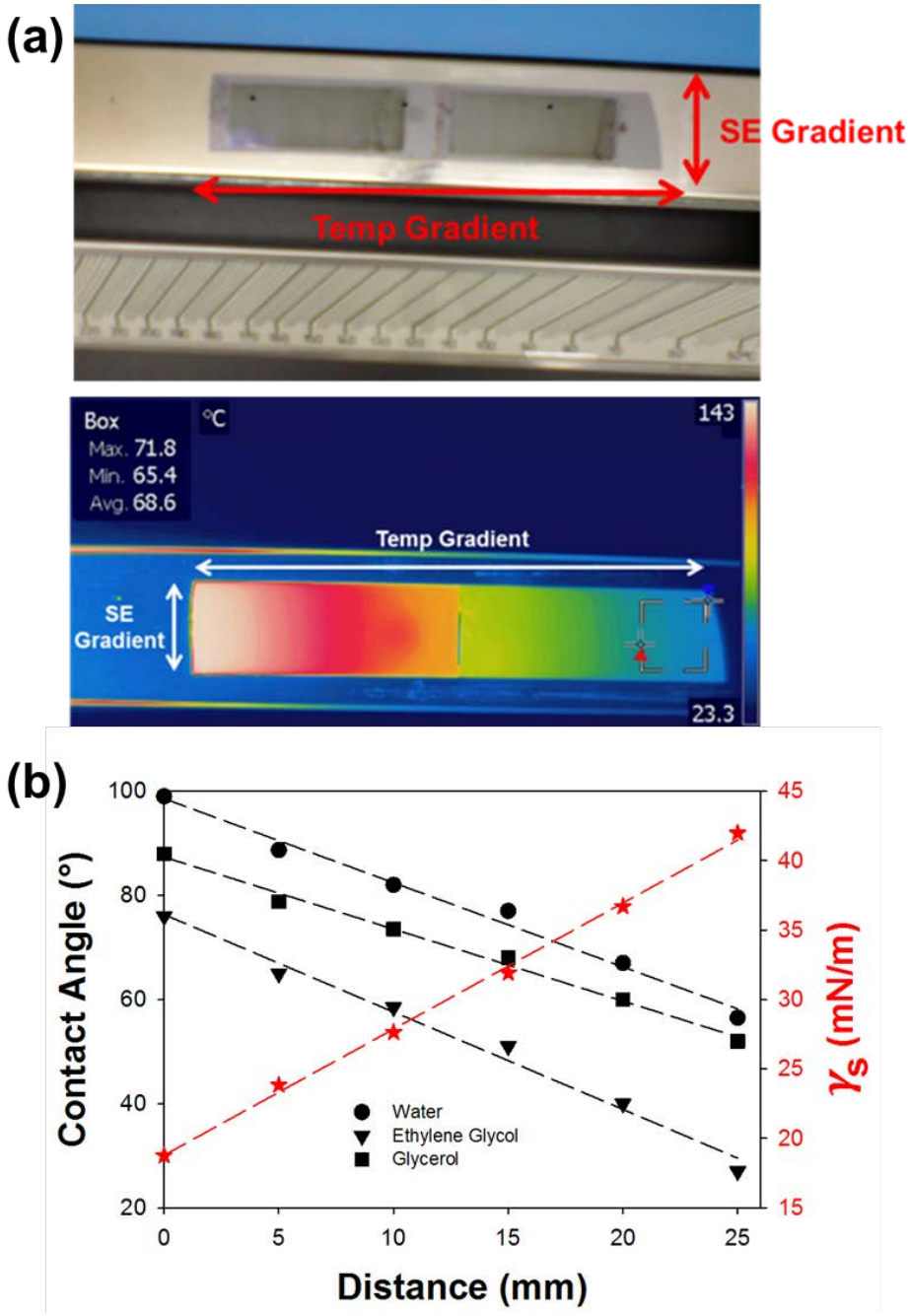

Figure S2 (a) Digital (top) and FLIR (bottom) images of experimental setup for dewetting of orthogonal surface energy and temperature gradients. The temperature is uniform in the direction parallel to the surface energy gradient. (b) Contact angles at 25°C using water, ethylene glycol, and glycerol (solid black symbols) to determine the substrate surface energy (red symbols) at different positions along the surface energy gradient.

S4. Substrate Surface Energies at Elevated Temperatures

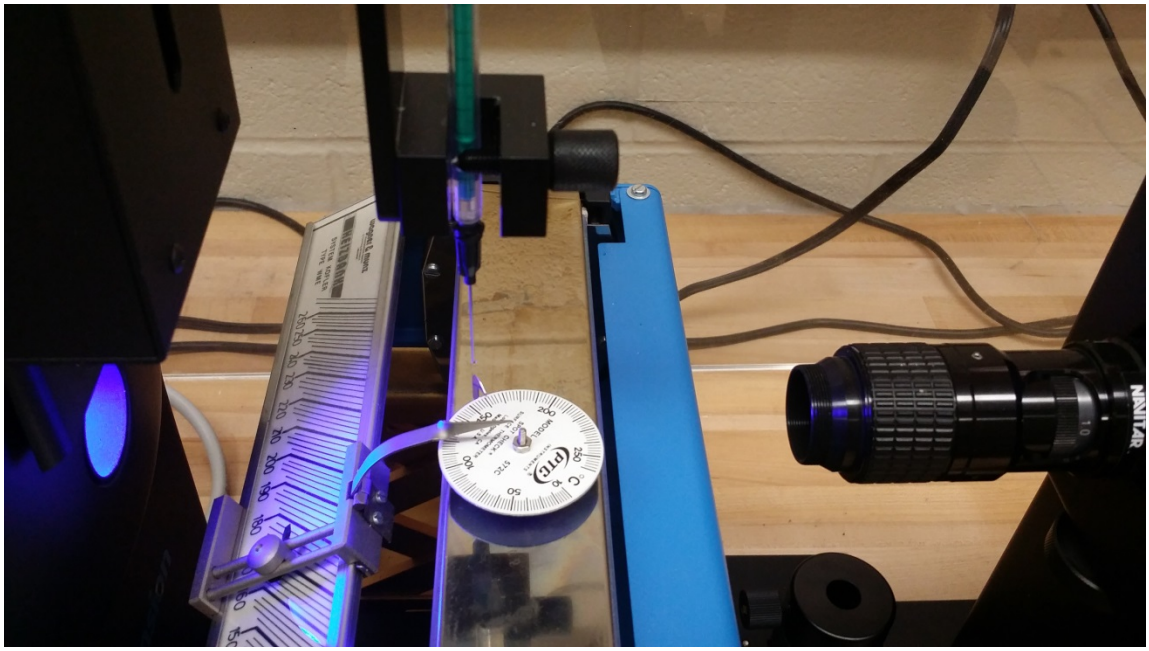

Figure S3 Contact angle measurements using ethylene glycol (b.p.=197.3°C) and glycerol (b.p.=290.0°C) at elevated temperatures. The temperature on the Kofler hot bench was calibrated using a 572CM direct contact spot check surface thermometer (PTC Instruments).

γ_S (mN/m) at 25°C	γ_S (mN/m) at 130-160°C
20.9	17.2
34.7	32.8
43.9	41.4

Table S1 Substrate surface energy (γ_S) to the *n*-octyltrichlorosilane functionalized silicon determined from contact angles (Equation S3) along different positions on the gradient. It is to note that the contact angles were similar between 130-160°C.

S5. Enlarged Map of Wetting-Dewetting Transition for Linear PS52k and Au20-PS50k

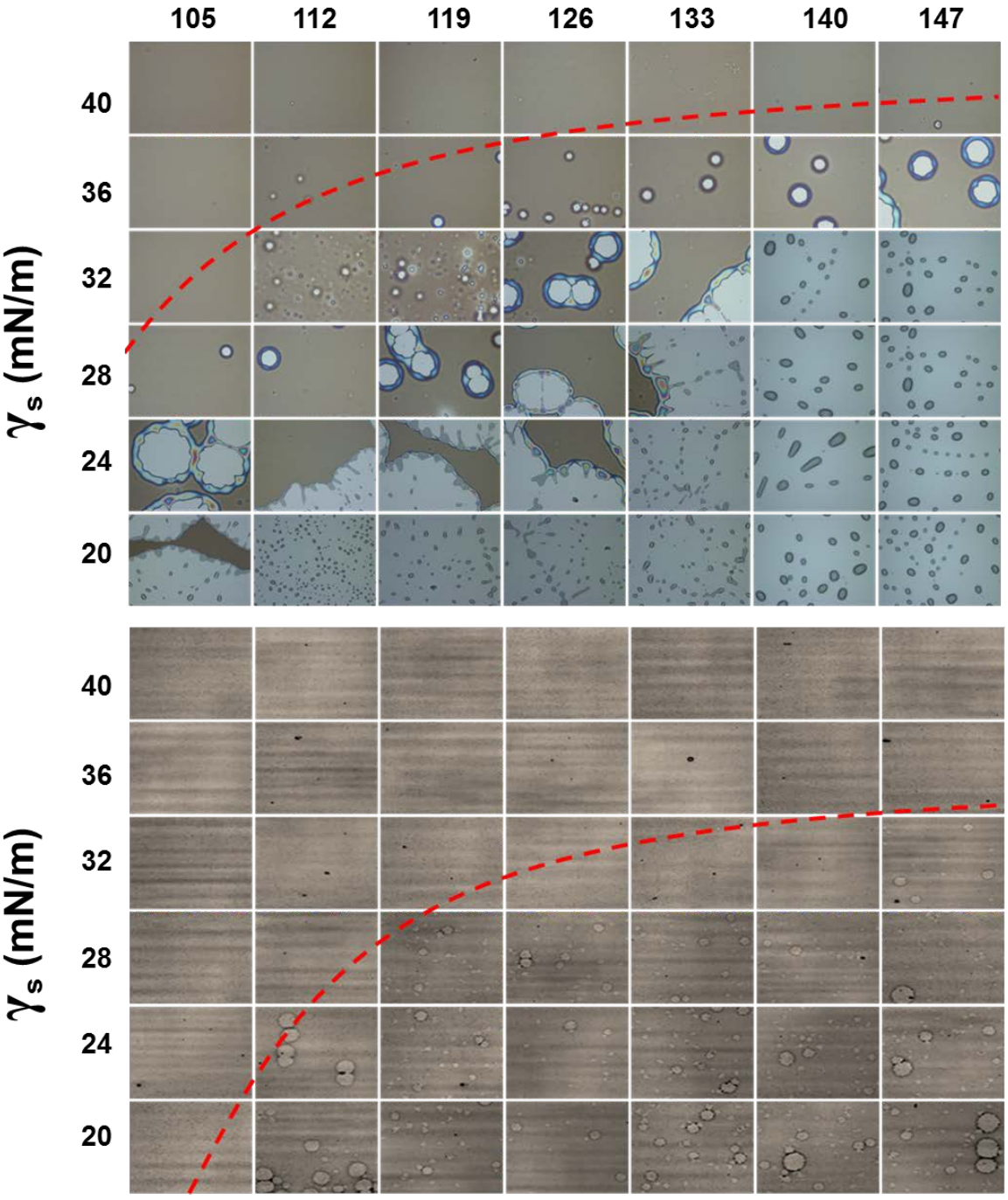

Figure S4 Enlarged map of wetting and dewetting regions from Figure 1 in main text for linear PS52k (top) and Au20-PS50k (bottom) with orthogonal substrate surface energy and temperature gradients.

S6. Wetting-Dewetting Transition for Linear PS11k and Au20-PS12k

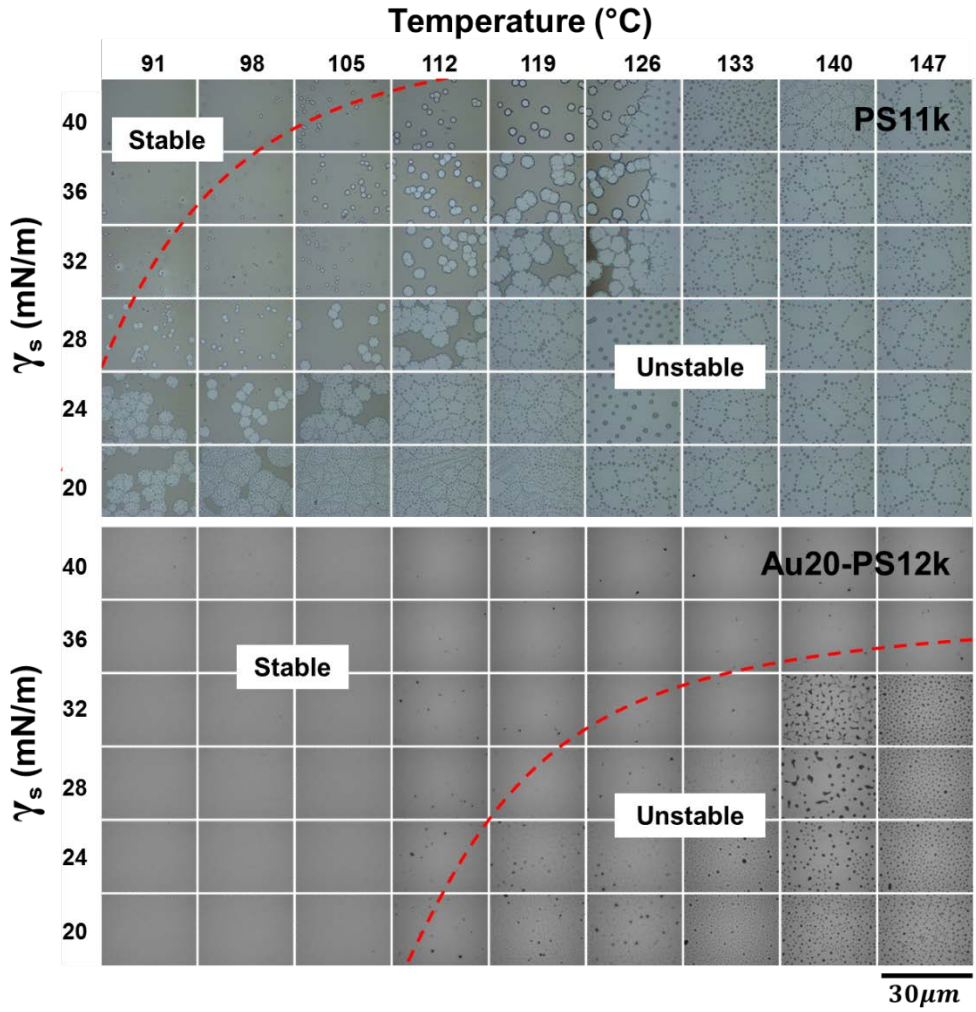

Figure S5 Map of wetting and dewetting regions for linear PS11k (top) and Au20-PS12k (bottom) with orthogonal substrate surface energy and temperature gradients. Scale bar for both samples is shown in the bottom right. The red dashed lines indicate the wetting-dewetting transitions.

S7. Wetting-Dewetting Transition for Linear PS21k and Au20-PS20k

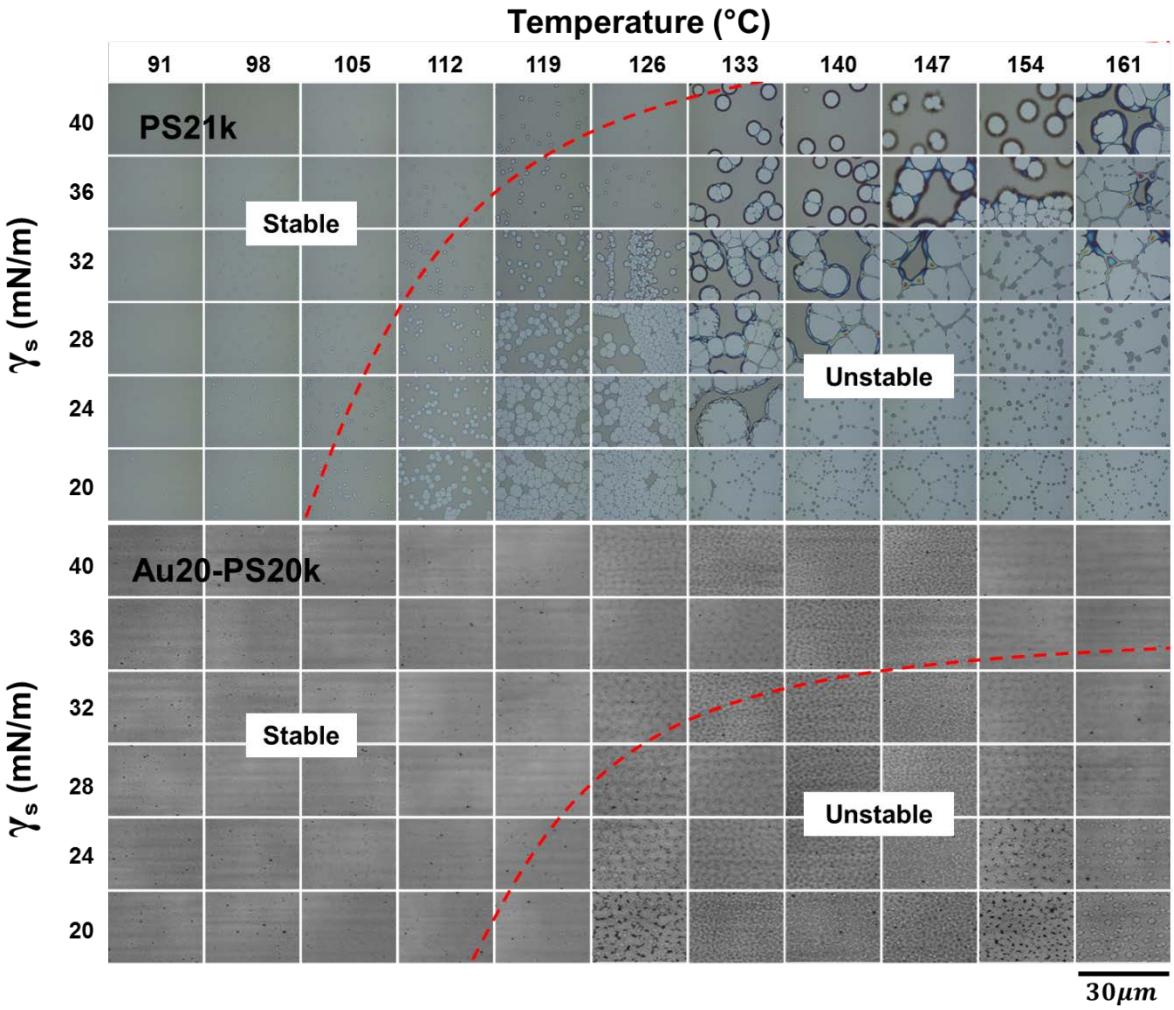

Figure S6 Map of wetting and dewetting regions for linear PS21k (top) and Au20-PS20k (bottom) with orthogonal substrate surface energy and temperature gradients. Scale bar for both samples is shown in the bottom right. The red dashed lines indicate the wetting-dewetting transitions.

S8. Wetting-Dewetting Transition for Linear PS52k and Au20-PS50k

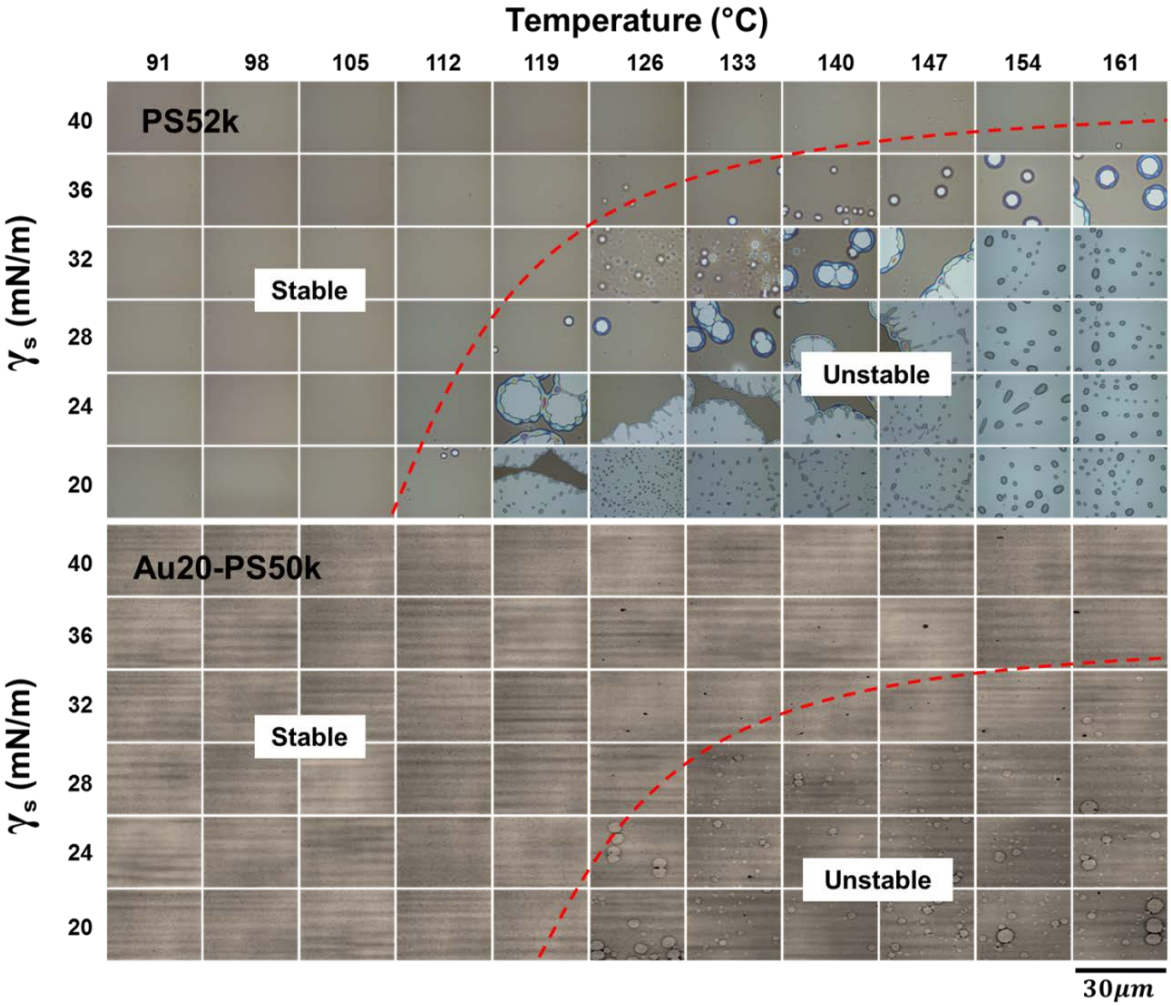

Figure S7 Map of wetting and dewetting regions for linear PS52k (top) and Au20-PS50k (bottom) with orthogonal substrate surface energy and temperature gradients. Scale bar for both samples is shown in the bottom right. The red line indicates the wetting-dewetting transition.

S9. Comparison of Wetting-Dewetting Transition for All AuNP-PS Thin Films

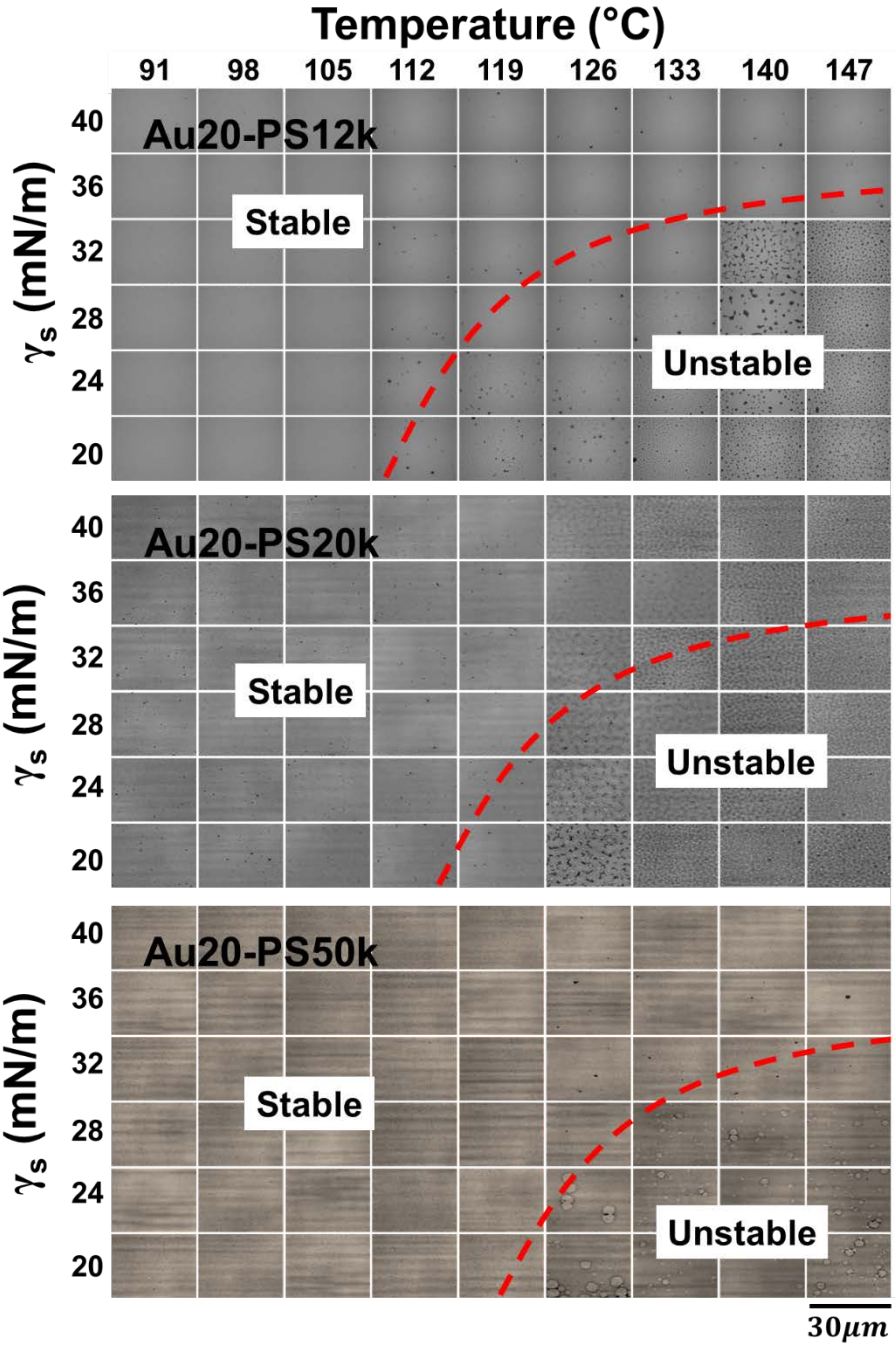

Figure S8 Map of wetting and dewetting regions for Au20-PS12k, Au20-PS20k, and Au20-PS50k with orthogonal substrate surface energy and temperature gradients. Scale bar for all samples is shown in the bottom right. The red line indicates the wetting-dewetting transition.

S10. Influence of Substrate Surface Energy Preparation on Wetting-Dewetting Transition

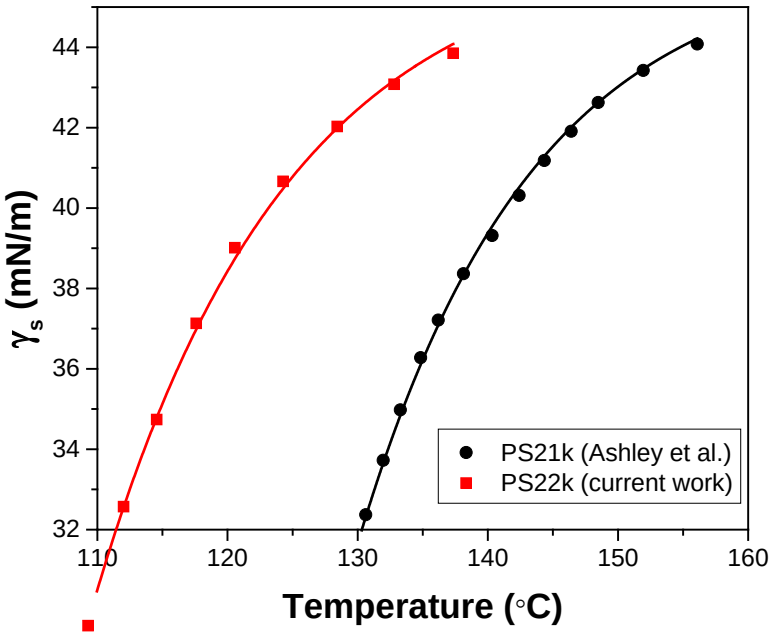

Figure S9 Wetting-dewetting transitions for linear PS22k used in this work (red) and PS21k (black, from Ashley et al.[4]). The transition occurs at much lower temperatures ($\Delta T \sim 20°C$) for the linear PS used in this work. The difference in the transition is attributed to variations in processing technique for substrate surface energy gradients, which alters the film-substrate interactions.

S11. Normalized Wetting-Dewetting Transition

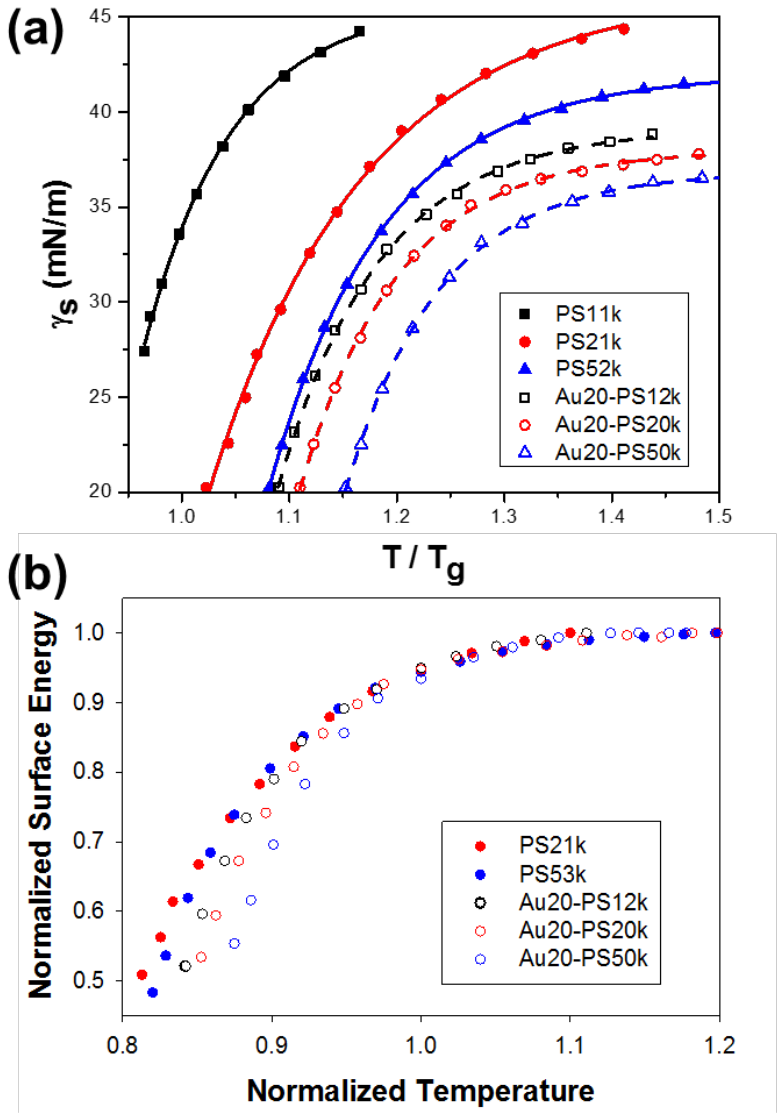

Figure S10 (a) Wetting-dewetting transitions for linear PS (filled symbols) and AuNP-PS (open symbols) thin films at various molecular weights normalized with T_g of each polymer. (b) Wetting-dewetting transitions normalized with the plateau regions of each stability curve. The plateau region is defined as the crossover value at high T when γ_s deviates from a constant value. A more detailed procedure about this normalization is described by Ashley et al.[4]. There is a clear shift to increased thermal and energetic stability from linear PS to PGN. It is interesting to note that the linear PS samples collapse into a single universal curve (consistent with those reported by Ashley[4]), whereas the PGNs do not show this universal behavior. The details of this still remains to be determined.

S12. Glass Transition Temperatures for linear PS and AuNP-PS

Sample	T_g (°C)
PS11k	94.0
PS21k	100.1
PS52k	100.5
Au20-PS12k	102.3
Au20-PS20k	103.2
Au20-PS50k	103.8

Table S2 Glass transition temperature of linear PS and AuNP-PS.

S13. Onset of Dewetting for Linear PS and AuNP-PS

Sample	γ_S Onset of Dewetting (Spreading Coefficients at 25°C) (mN/m)	γ_S Onset of Dewetting (Orthogonal and T at 150°C) (mN/m)
PS11k	40.6	41.0
PS21k	39.9	39.3
PS52k	39.2	38.6
Au20-PS12k	36.7	35.8
Au20-PS20k	36.7	35.6
Au20-PS50k	36.2	35.0

Table S3 Summary of onset of dewetting from contact angle experiments at 25°C and from orthogonal surface energy and temperature gradients at 150°C.

S14. REFERENCES

1. Che, J.; Park, K.; Grabowski, C. A.; Jawaid, A.; Kelley, J.; Koerner, H.; Vaia, R. A. Preparation of Ordered Monolayers of Polymer Grafted Nanoparticles: Impact of Architecture, Concentration, and Substrate Surface Energy. *Macromolecules* **2016**, *49*, 1834−1847.
2. Genzer, J.; Efimenko, K.; Fischer, D. A. Molecular Orientation and Grafting Density in Semifluorinated Self-Assembled Monolayers of Mono-, Di-, and Trichloro Silanes on Silica Substrates. *Langmuir* **2002**, *18*, 9307-9311.
3. Bhat, R. R.; Genzer, J. Tuning the Number Density of Nanoparticles By Multivariant Tailoring of Attachment Points on Flat Substrates. *Nanotechnology* **2007**, *18*, 025301, 1-6.
4. Ashley, K. M.; Raghavan, D.; Douglas, J. F.; Karim, A. Wetting-Dewetting Transition Line in Thin Polymer Films. *Langmuir* **2005**, *21*, 9518-9523.
5. Ohno, K.; Morinaga, T.; Takeno, S.; Tsujiii, Y.; Fukuda, T. Suspensions of Silica Particles Grafted With Concentraed Polymer Brush: Effects of Graft Chain Length on Brush Layer Thickness and Colloidal Crystallization. *Macromolecules* **2007**, *40*, 9143-9150.
6. Owens, D.K.; Wendt, R.C. Estimation of the Surface Free Energy of Polymers. *J. Appl. Polym. Sci.* **1969**, *13*, 1741-1747.
7. Fowkes, F. M. "Chemistry and Physics of Interfaces," American Chemical Society, Washington, D.C. (1965), 1-12.
8. Good, R. J. Contact Angle, Wetting, and Adhesion - A Critical Review. *J. Adhesion Sci. Technol*. **1992**, *6*, 1269-1302.
9. van Oss, C. J.; Chaudhury, M. K.; Good, R. J. "Interfacial Lifshitz-van der Waals and Polar Interactions in Macroscopic Systems," *Chem. Rev.* **1988**, *88*, 927-941.
10. Hollander, A. "On the Selection of Test Liquids for the Evaluation of Acid-Base Properties of Solid Surfaces by Contact Angle Geometry," *J. Coll. Interf. Sci* **1995**, *169*, 493-496.